Atmospheric Research 327 (2026) 108340



Contents lists available at ScienceDirect

Atmospheric Research

journal homepage: www.elsevier.com/locate/atmosres





Emergence of autumn rainy season in Korea due to tropical cyclone influence

Hee-Ae Kim [a], Chang-Hoi Ho [a,b,*], Minhee Chang [c,d], Jinwon Kim [b]

[a] School of Earth and Environmental Sciences, Seoul National University, Seoul, Republic of Korea
[b] Department of Climate and Energy Systems Engineering, Ewha Womans University, Seoul, Republic of Korea
[c] Environmental Planning Institute, Graduate School of Environmental Studies, Seoul National University, Seoul, Republic of Korea
[d] Climate Tech Center, Seoul National University, Seoul, Republic of Korea

ARTICLE INFO

Keywords:
Autumn rainfall
Tropical cyclone
Western North Pacific subtropical high
Heavy rainfall
Korea

ABSTRACT

Autumn in Korea, following the peak rainy season in summer, is of a great importance as it coincides with the intensive harvesting of crops and fruits. Hence, autumn rainfall critically affects agricultural production in Korea. This study shows the emergence of new rainfall peaks in autumn, leading to potentially significant agricultural damages. In the monthly period from September 10 to October 10, the total rainfall in the recent period (150 mm for 1998–2023) has increased by 44 mm compared to the previous period (106 mm for 1979–1997), averaged over 61 stations. Heavy rainfall days ($\geq$ 100 mm day^{-1}) have also occurred more frequently. The most plausible mechanism for these changes is the delayed retreat of the western North Pacific subtropical high in autumn which results in westward shift of tropical cyclone (TC) tracks and increased number of days on which Korea is affected by TCs. In addition, rising sea surface temperatures (0.5–1.0°C) in the western North Pacific and the South China Sea appear to be related to increased TC-induced heavy rainfall in Korea. Enhanced low-level moisture transports from these warm oceanic areas toward Korea, combined with upper-level wind divergence, are likely to have intensified the conditions for the TC-induced heavy rainfall. This study highlights the need for further research and public awareness of the changing autumn rainfall patterns and their impacts on agriculture and infrastructure.

1. Introduction

Global warming has significantly affected tropical cyclone (TC) activities, resulting in alteration of frequencies, tracks, and intensities (Chand et al., 2022; Knutson et al., 2020; Sobel et al., 2016; Wu and Wang, 2004) while also shifting their seasonality on the global scale. Shan et al. (2023) showed that the occurrence of intense TCs in the Northern Hemisphere have advanced significantly at a rate of 3.7 days per decade. This trend is attributed to the early emergence of high ocean heat capacity due to ocean warming. This earlier occurrence of intense TCs during summer raises the likelihood of extreme rainfall events overlapping with TC-induced rainfall, potentially leading to catastrophic impacts. In contrast to this global trend, East Asia has experienced increased TC activities in autumn (Basconcillo and Moon, 2022; Yao et al., 2020). In particular, TCs affecting Korea has decreased in summers but increased in autumns (Na and Jung, 2020).

The delayed occurrence of TCs affecting Korea in autumn has exacerbated the economic losses in the agricultural sector. Statistics from the Ministry of the Interior and Safety (MOIS) of Korea show that over the past two decades (2003−2022), the average annual economic losses caused by autumn TCs (US $1.3 billion) exceeded those caused by summer TCs (US $911 million). Furthermore, the frequency of severe rainfall damage such as floods, landslides, infrastructure destructions, and agricultural losses, by TCs is substantially larger in autumn than in summer (219 in autumn vs. 117 in summer over the past two decades) (MOIS, 2024). More than 50% of the total losses by autumn TCs is primarily related to the loss in farmlands and agricultural products. This is particularly important as the weather in autumn critically affects the yield of major agricultural products such as rice, vegetables and fruits in Korea.

Changes in autumn TC activities over East Asia have been suspected as a potential driver of increased autumn rainfall in the region (Choi et al., 2010; Do et al., 2023; Qian et al., 2002; Son et al., 2016). Choi et al. (2010) and Do et al. (2023) reported increases in the autumn-mean

* Corresponding author at: Department of Climate and Energy Systems Engineering, Ewha Womans University, Seoul 03760, Republic of Korea.
E-mail address: hoch@ewha.ac.kr (C.-H. Ho).

https://doi.org/10.1016/j.atmosres.2025.108340
Received 22 February 2025; Received in revised form 25 June 2025; Accepted 3 July 2025
Available online 4 July 2025
0169-8095/© 2025 The Authors. Published by Elsevier B.V. This is an open access article under the CC BY-NC license (http://creativecommons.org/licenses/by-nc/4.0/).

rainfall in Korea and suggested that enhanced TC activities may be a contributing factor. Qian et al. (2002) also hypothesized that the increase in autumn rainfall over China should be linked to TC activity, although their study does not present direct analytical evidence to support the claim. Since rainfall in East Asia is predominantly concentrated in summer due to the East Asian summer monsoon, the increase in autumn rainfall (typically a drier season) has received relatively limited research attention. More recently, however, Son et al. (2016) found that increased September rainfall in Korea is correlated with the change in TC tracks influenced by the Niño 3 sea surface temperature variations, providing an important clue for the link between the TC activity and rainfall in Korea during autumn.

In general, changes in the TC-induced rainfall are closely influenced by the atmospheric and oceanic conditions. As TCs typically follow the steering flow in the mid-to-upper troposphere (around 500 hPa), the extent of the Western North Pacific Subtropical High (WNPSH) is considered to critically affect TC tracks, and in turn are closely linked to the rainfall distribution in East Asia (Nakamura et al., 2017; Wu et al., 2020). Climate variabilities such as the El Niño–Southern Oscillation (ENSO) and the Pacific Decadal Oscillation (PDO) also play a critical role in modulating the genesis locations and trajectories of TCs, thereby affecting the regions of TC-related rainfall (Chan, 2000; Son et al., 2016; Zhang et al., 2012). When upper-level mid-latitude troughs overlap with TC tracks, they can enhance vertical motion within the TC system, leading to intensified rainfall (Kim et al., 2006). In addition, warmer sea surface temperature (SST) increases the supply of heat and moisture to TCs, further enhancing rainfall and potentially altering the spatial extent of TC-induced rainfall (Lin et al., 2015). In recent years, numerous studies have reported that the change in TC activities over East Asia becomes increasingly evident in response to changes in both atmospheric and oceanic conditions (Kim et al., 2005; Park et al., 2014; Wu et al., 2005; Zhao et al., 2018).

Although notable changes in TC activities across East Asia and increases in the autumn rainfall in Korea have been observed in recent years, few studies have clearly established the connection between these two. Moreover, despite the continued rise in damages by autumn TCs, the severity of the issue has not received sufficient attention. This study aims to analyze the characteristics of the autumn rainfall increases in Korea and to identify the mechanisms underlying this trend. In addition, the broader implications of these changes are discussed in the context of climate change, with the goal of enhancing scientific understanding and raising public awareness of the influence of TCs on shifting rainfall patterns in Korea.

2. Data

2.1. Automated Synoptic Observing System (ASOS)

This study analyzes the daily rainfall data observed at the ASOS stations managed by the Korea Meteorological Administration (KMA). A total of 61 stations are selected to ensure a even regional representation across the entire administrative area of Korea, including major islands such as Jeju-do and Ulleung-do (Fig. 1). It should be noted that many previous studies exclude the data from these islands due to their geographical isolation and unique climatic characteristics (e.g., Choi et al., 2018). These two islands are included in this study because they often serve as key observation points for TCs either approaching or making landfall in Korea. The primary variable is the daily rainfall measured as the total accumulation from 0 to 24 h Korea Standard Time (KST). Only the data of $\geq$1 mm day^{-1} are used in the analysis. The data covers the 45-year period from 1979 to 2023. Although it is technically possible to extend the analysis to earlier years, 1979 is chosen as the starting point to match the availability of high-quality reanalysis data.

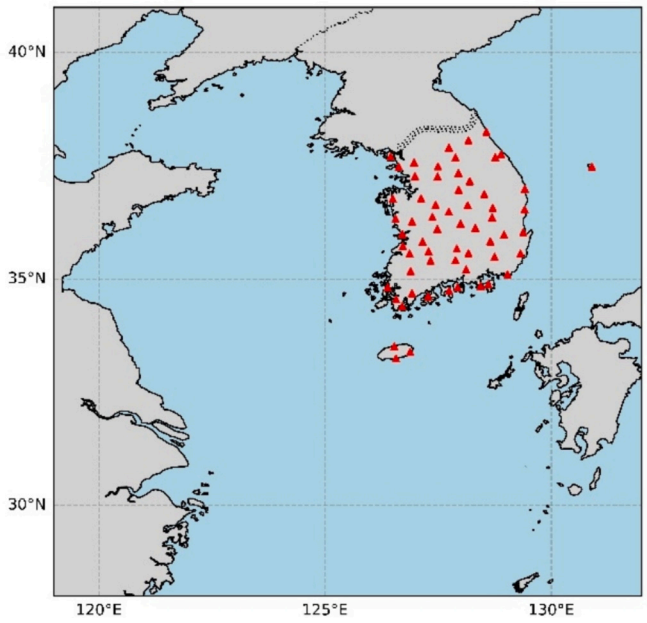


Fig. 1. Map illustrating the emergency zone used to define tropical cyclones (TCs) affecting Korea. The red triangles indicate the 61 Automated Synoptic Observing Systems (ASOS) stations used in the analysis. (For interpretation of the references to colour in this figure legend, the reader is referred to the web version of this article.)

2.2. ERA-5 reanalysis

The fifth-generation atmospheric reanalysis of the European Centre for Medium-Range Weather Forecasts (ERA5) for 1979–2023 is analyzed to examine the environmental conditions that modulate autumn rainfall. The raw data provides hourly values at spatial resolutions of 0.25° × 0.25°; this study utilizes the 6-h data to obtain the large-scale climatic variations. To investigate the dynamical atmospheric processes related to rainfall, this study utilizes SST, specific humidity at the 850-hPa level, geopotential height at the 500- and 200-hPa levels, and the zonal- and meridional winds at the 850- and 200-hPa levels. In addition, vertically-integrated moisture flux divergence (VIMFD) is calculated using the specific humidity and horizontal wind at isobaric levels from 1000 hPa to 500 hPa in 100-hPa intervals.

2.3. Best track data

The Regional Specialized Meteorological Center (RSMC) Tokyo Best Track dataset provided by the Japan Meteorological Agency are used to adjust TC-affected date. For consistency with other datasets, the study includes the TCs that affected Korea between 1979 and 2023. The KMA also provides Best Track data for TCs affecting Korea, but its record goes back to only 2013, so it is necessary to rely on the RSMC Tokyo dataset. This dataset provides comprehensive information on TCs in the western North Pacific and the South China Sea at 6-h intervals, including tracks, central pressures, maximum wind speeds, and intensities. The RSMC data classifies TCs into categories such as tropical depressions, tropical storms, and typhoons, in conjunction with the records on their development stages including the tropical cyclone, extratropical cyclone, or dissipation. It also documents the changes in their tracks and intensities over time.

3. Method

3.1. Definition of TCs affecting Korea and their affected stations

This study examines the TCs that approached or made landfall in

Korea with a focus on identifying their impact periods. The analysis requires information on the TC identification number and the start and end dates of their impact period. These data are sourced from two primary references: (1) the Typhoon White Book, which documents TC tracks affecting Korea from 1904 to 2010, and (2) the annual analysis report on TCs affecting Korea since 2011 (Chang et al., 2023). Adjustments to the start and end dates of TC-affected periods are necessary due to the changes in the criteria for defining the TC-affected area. Until 2010, a TC was considered to affect Korea if it was within the region bounded by 32°N–40°N and 120°E–138°E. However, in 2011, the definition was revised to a new emergency zone that includes areas north of 28°N and west of 132°E (Fig. 1). To ensure consistency across the entire study period, TC-affected day is redefined based on the time at which a TC entered the updated emergency zone. Rainfall recorded at ASOS stations within this zone during the TC's presence is defined as the TC-induced rainfall.

To assess the extent of TC impacts during the identified periods, the number of affected stations is calculated following the method of Park et al. (2015), which builds on the approach of Donat et al. (2011). In this framework, a station is considered TC-affected if either the daily maximum wind speed or the accumulated rainfall exceeds a defined threshold. As the present study focuses on the rainfall, only the threshold for daily accumulated rainfall, 30 mm, are applied. This threshold corresponds to the average of the 90th-percentile value at each station and is regarded as the lower limits to incur losses.

3.2. Vertically integrated moisture flux divergence (VIMFD)

VIMFD represents the vertical integration of the horizontal divergence of moisture flux within the atmospheric column. It serves as a useful diagnostic variable for identifying areas of moisture flux convergence (negative values) and divergence (positive values), which are closely associated with rainfall. Moisture flux is defined as the product of the horizontal wind vector ($\vec{V}$) and specific humidity (q), representing the amount of moisture transported per unit area per unit time. In this study, VIMFD is calculated using the following equation:

$$\mathrm{VIMFD} = \nabla\cdot\left(\frac{1}{g}\int_{p1000}^{p500}\vec{V}q\,dp\right)$$

where g is gravitational acceleration, and p denotes the pressure. The integration is performed over pressure levels from 1000 hPa to 500 hPa at 100-hPa intervals, using 6-hourly ERA5 reanalysis data. By analyzing VIMFD during TC-affected periods, this study aims to capture the spatial structure of anomalous moisture flux convergence and explore its role in modulating TC-induced rainfall over Korea.

3.3. Statistical method

As the present study demonstrates interdecadal shifts in the atmospheric and oceanic environments associated with TC activity in East Asia, an objective statistical method should be applied to identify whether these shifts are statistically significant. Here, the student's *t*-test is used, which is one of the widely used statistical tools. The test calculates a t-statistic based on the difference between the sample means, standard deviations, and the sample sizes. If the resulting *p*-value is less than a chosen significant level, it implies that there is statistically significant difference between the two groups. Although this test assumes that the data area approximately normally distributed and that the variances of the two groups are equal, the present study use Welch's t-test which can be used when this assumption is violated.

4. Autumn rainfall and its relationship with TC

4.1. Emergence of autumn rainy season

Climatologically, rainfall in Korea is concentrated in summer, with two distinct peaks: the primary rainy season (from late June to late July; called *Changma*) and the secondary rainy season (from early August to early September; called *Autumn Changma*) (Ho et al., 2004; Ho et al., 2025). However, the present study focuses on the rainfall that occurs after the end of the summer rainy season. Fig. 2a shows the interannual variations in daily mean rainfall for two periods: a past period (P1, 1979–1997) and a recent period (P2, 1998–2023). The division at 1997/98 is based on previous findings by Choi et al. (2010) and Moon et al. (2011), which suggest a regime shift in Korean summer rainfall around that time.

In Fig. 2a, a distinct rainfall peak in P2 appears after September 10 with the maximum value of 8 mm day^{-1}, while this early autumn rainfall peak is absent in P1. The September rainfall peak in P2 is smaller than those of the two summer rainy periods but is still prominent, especially considering that rainfall gradually decreases from September into dry autumn in P1. Based on this change, the period from September 10 to October 10, during which this new peak occurs, is defined as the *autumn rainy season*. This period is identified by locating the two rainfall peaks that exceed 5 mm/day and occur after the termination of the secondary rainy season. The boundaries are determined using local minima that mark the start and end of the peak period. The mean daily rainfall during this season increases by 1.8 mm day^{-1} (55%) in P2 (4.9 mm day^{-1}) from P1 (3.1 mm day^{-1}). Comparing the long-term rainfall increases between P1 and P2 for the primary and secondary rainy seasons are 1.0 mm day^{-1} (12%) and 0.6 mm day^{-1} (8%), respectively, the rainfall increased in the newly emerging autumn rainy season is prominent.

Fig. 2b shows the time series of total rainfall from September 10 to October 10 (monthly rainfall hereafter) for the period 1979–2023. The rainfall in the period ranges from 40 to 200 mm month^{-1} over the analysis period, with a noticeable increase in the inter-decadal

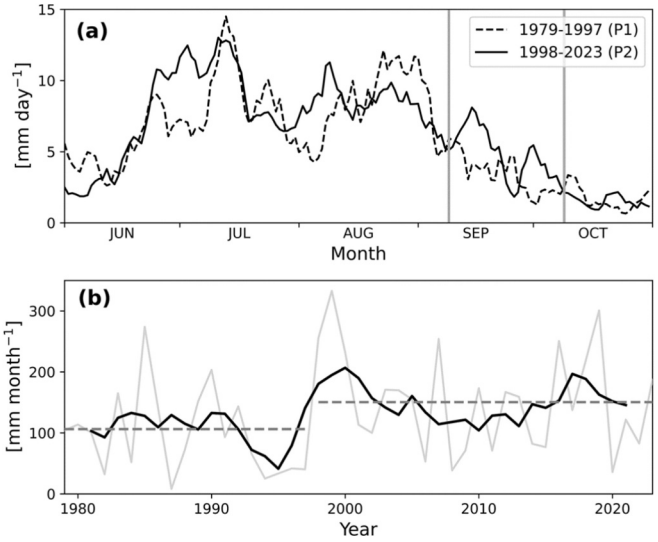


Fig. 2. (a) Comparison of intra-annual variations of the 5-day moving average of daily rainfall (unit: mm day^{-1}) between the 1979–1997 (P1, dashed) and 1998–2023 (P2, solid). The vertical lines in (a) mark the start (September 10) and end (October 10) date of the autumn rainy season. (b) Interannual variation in the total rainfall (unit: mm month^{-1}) for autumn rainy season during 1979–2023 (grey line), with a 5-year moving average (black line). The dashed horizontal lines indicate the mean values for the two periods P1 and P2. The difference in the mean values between the two periods is statistically significant at the 99% confidence level based on a two-sided Student's *t*-test.

variability in recent decades. In particular, there is a distinct jump in the monthly rainfall around 1997/98. In P2, the average monthly rainfall is 150 mm, a 44 mm increase from 106 mm in P1. The change-point analysis reveals an obvious shift around 1997/1998 (not shown). This timing coincides with the regime shift previously identified in summertime rainfall by Choi et al. (2010) and Moon et al. (2011), suggesting that a similar shift also occurred in autumn rainfall. Such abrupt changes in Korea have been reported for temperature (Choi et al., 2018); however, the changes in the autumn rainfall have not been reported.

The increase in the average rainfall is accompanied by more frequent extreme events (Ho and Kang, 1988; Ho et al., 2025). Fig. 3 shows the interannual variation in the number of heavy rainfall days ($\geq$ 100 mm day^{-1}) (Fig. 3a) and the maximum daily rainfall (Fig. 3b) in the autumn rainy season for each year. Despite considerable interannual variability, the frequency has increased significantly since the late 1990s. Before the late 1990s, only one year (1985) shows over 3 days with heavy rainfall events; since then, the year of more than 4 heavy rainfall days occur, on average, once every four years. The annual average (median) number of heavy rainfall days also shows a significant increasing trend. In P1, the average (median) is 1.1 (1.0) days per year, while in P2, it rises to 2.5 (2.5) days per year, representing an increase in the number of heavy rainfall days of about 2.3 (2.5) times. In addition to the number of heavy rainfall days, the rainfall intensity also has increased significantly (Fig. 3b). The difference in rainfall intensity between P1 and P2 is statistically significant at the 95% confidence level. Before the late 1990s, the annual average (median) of the maximum daily rainfall is 141 mm day^{-1} (130 mm day^{-1}), while it rises to 216 mm day^{-1} (196 mm day^{-1}) after the late 1990s. This represents an increase of 75 mm day^{-1} (66 mm day^{-1}), corresponding to a 53.2% (50.8%) rise. While some years of exceptionally large daily rainfall of $\geq$400 mm day^{-1} (e.g., 1998, 2003, 2007) affect the averages, it is noteworthy that the daily maximum rainfall exceeding 100 mm day^{-1} occurred almost every year.

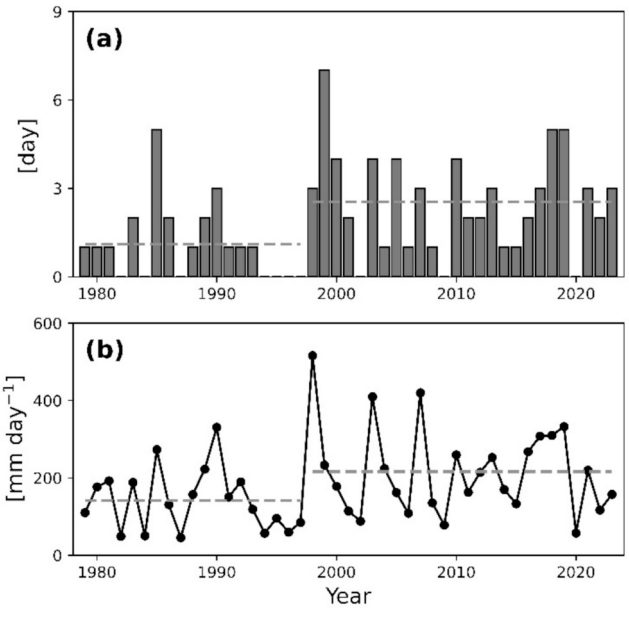


Fig. 3. Annual variation of (a) the number of heavy rainfall days ($\geq$ 100 mm day^{-1}) and (b) the maximum daily rainfall for the autumn rainy season of 1979–2023. The dashed horizontal lines in each panel represent the mean values for the two periods (P1 and P2). In (a) and (b), the difference in the mean values between the two periods is statistically significant at the 90% confidence level based on a two-sided Student's *t*-test.

4.2. Influence of autumn tropical cyclone

Why has the autumn rainfall increased in P2? It should be noted that autumn is minimally affected by convective systems associated with the East Asian summer monsoon or synoptic conditions favorable for heavy rainfall (Ho and Kang, 1988; Kim et al., 2018; Qian et al., 2002). Instead, previous studies speculated that the autumn rainfall in Korea is mainly determined by TC rainfall with limited contribution from frontal rainfall (Rha et al., 2005; Yang, 1999). The contribution of TCs to the emergence of the autumn rainy season in P2 is demonstrated in the following.

Fig. 4 shows (a) the intra-annual variation of the 5-day moving average of TC-induced rainfall and (b) the number of TC-affected days averaged over P1 and P2. While the TC-induced rainfall amount in P2 is smaller than in P1 for mid-to-late August (this overlaps with the secondary summer rainy season), the TC-induced rainfall for the autumn rainy season is much larger in P2 than in P1, especially in mid-to-late September (Fig. 4a). The TC-induced rainfall peak (Fig. 4a) also coincides well with the total rainfall peak in the autumn rainy season (Fig. 2a). In the autumn rainy season, the TC-induced 5-day moving average rainfall increases from 0.6 mm day^{-1} in P1 to 1.9 mm day^{-1} in P2, accounting for 72% of the total rainfall increase (1.8 mm day^{-1}) at the 95% confidence level. This implies that the increase in the TC-induced rainfall drives the total autumn rainfall increase in P2.

What changes in TCs increased autumn rain in Korea? One possibility is higher frequency of TCs approaching Korea, which can enhance moisture transport and, subsequently, rainfall. Fig. 4b shows the number of days on which Korea is affected by TC in the period from June to October. Overall, during the two active TC-affected months from late July to mid-September, TCs affect Korea for about 11 days per decade. Significant differences are found between P1 and P2 during these two months. From P1 to P2, the number of TC-affected days in the mid- to late August period decreases by 0.9–2.1 days per decade, while it increases by up to 3.9 days per decade in the first half of September. This period also exhibits the most pronounced increase in TC-induced rainfall (Fig. 4a), which significantly contributes to the overall rise in the total rainfall (Fig. 2a). The rainfall increases between P1 and P2 in the period from late September to early October, although it is not as pronounced

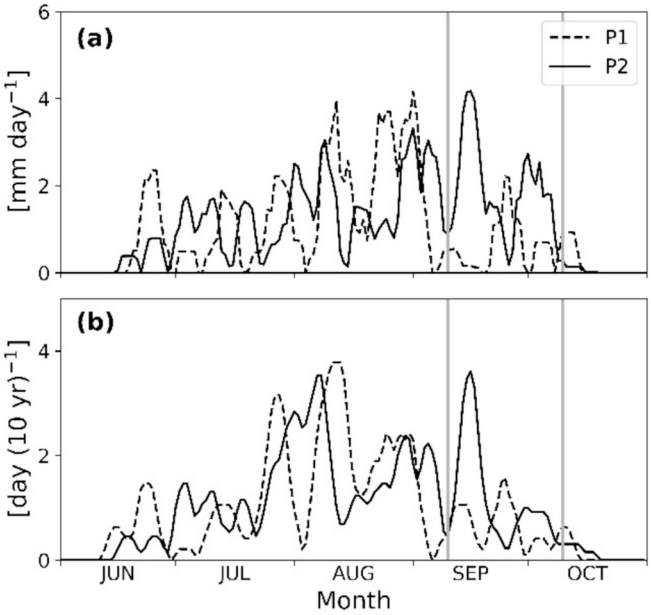


Fig. 4. (a) 5-day moving averages of TC-induced daily rainfall averaged across the 61 stations and (b) TC-affected days per decade for P1 (dashed) and P2 (solid). In (b), a TC-affected day is defined as the number of days when TCs enter within the TC emergency zone. The two vertical lines represent September 10 and October 10, as indicated in Fig. 2a.

as in the early to mid-September period (Fig. 4a), is also accompanied by the increase in the number of TC-affected days (Fig. 4b).

The relationship between the autumn rainfall and the TC-induced rainfall is evident not only in the daily climatology but also in the interannual variations (compare Fig. 2b and Fig. 5). Examining the 5-year moving average of the annual TC-induced rainfall averaged over the 61 stations for the autumn rainy seasons of the entire 45-year period (thick line in Fig. 5), reveals an overall increase after the late 1990s (i.e., P2). This contrasts the TC-induced rainfall in P1 where the average rainfall remains below 40 mm month^{-1}. Annual TC-induced rainfall amounts (light line) show a significant jump with peaks above 100 mm month^{-1} in P2. Like the total rainfall (Fig. 2b), the TC-induced rainfall shows prominent peaks around 2000 and in the late 2010s. Even in the period between these two peaks (the early 2000s to the late-2010s), rainfall is slightly above or comparable to that in P1. The annual variations in the TC-induced rainfall resembles the total rainfall which also shows two peaks at around 2000 and in the late-2010s. Furthermore, the correlation coefficient between the annual time series of the total and TC-induced rainfall (i.e., the two light lines in Figs. 2b and 5) is 0.78 at the 95% confidence level. In contrast, an analysis of the non-TC rainfall based on the same dataset (not shown) shows no clear increasing or decreasing trend, as the non-TC rainfall generally remains around 100 mm month^{-1} throughout the entire period except for a brief decrease in the mid-1990s. This further supports the fact that the recent changes in the total autumn rainfall are closely linked to the TC-induced rainfall.

The annual variations in the TC-induced rainfall appear to be closely related to the variations in the TC-affected days. Fig. 5 (bars) shows that over three TC-affected days occur for a year in 1991, 1999, and the period from the late 2010s to the early 2020s, coinciding with rainfall peaks. Nevertheless, the increase in the TC-affected days alone cannot explain the changes in the autumn rainfall. For example, in 2007–2008 and 2012–2013, the number of TC-affected days is relatively small (2 days per year), but the TC-induced rainfall exceeds 100 mm month^{-1}, much larger than the rainfall in the years of the same number of TC-affected days before 1997. This discrepancy suggests that the changes in TC-induced rainfall are not solely driven by the number of TC-affected days but may also involve shifts in other TC-related characteristics such as rainfall intensity or the spatial extent of TC impacts.

The relationship between TC-affected days and TC-induced rainfall shown in Fig. 5 prompts an examination of whether the intensity of TC-induced rainfall has changed significantly over time. The number of TC-induced heavy rainfall days and the corresponding maximum rainfall intensity (Fig. 6a and b) show that the average number of the TC-induced heavy rainfall days increases from 0.3 in P1 to 1.0 in P2 (3.3 times), while the maximum daily rainfall increases from 61 mm day^{-1} to 130 mm day^{-1} (2.1 times). Both increases are statistically significant at the 90% confidence level. The difference in their mean values between P1 and P2 are larger than the total rainfall difference for the same period (Fig. 3). In addition, extreme rainfall events of daily rainfall over 300 mm become more frequent after 1997, highlighting the intensification of extreme weather phenomena associated with TCs during P2.

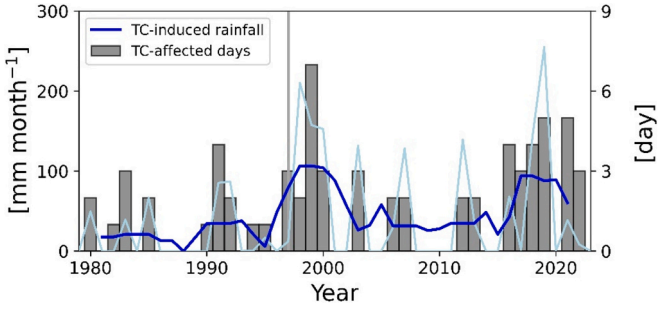


Fig. 5. TC-induced rainfall (light blue line, left y-axis) with its 5-year moving average (thick blue line, left y-axis) and the number of days (bar, right y-axis) with TC across the 61 stations during the autumn rainy season. A TC-affected day is defined when one of the 61 stations is influenced by TC. The vertical line shows the division of P1 and P2 based on the year 1997. (For interpretation of the references to colour in this figure legend, the reader is referred to the web version of this article.)

The risks posed by autumn TCs are not limited to more frequent heavy rainfall days. Fig. 6c illustrates the annual number of stations affected by TCs during the autumn rainy season when Korea is affected by the TCs that brought heavy rainfall. Fig. 6c clearly shows a large increase in the number of TC-affected stations after 1997. In P1, the number of stations affected by TCs rarely exceeds 100 per decade while seven years are affected by more than 100 stations in P2. The overall trend indicates an increase of 6.1 affected stations per decade. Considering that there are a total of 61 observation stations, this corresponds to an increase of about 10% per decade in the area affected by the TCs bringing heavy rainfall.

4.3. Climatological changes in TC tracks and environmental factors

The increase in the number of TC-affected days in Korea, along with the associated increase in rainfall and the expansion of the TC-affected area, can be attributed to the changes in the physical properties of TCs, such as intensity, track, and speed. Among these, this study focuses on the changes in TC tracks. Ho et al. (2004) reported westward shifts in TC tracks in summer (June–September), which are closely linked to the expansion of the WNPSH. In this study, we limit our analysis to the autumn rainy season, examining the 500-hPa geopotential height over the western North Pacific, an important indicator of weather and climate in East Asia, along with the TC tracks in P1 and P2.

Fig. 7 illustrates the differences in the TC track frequency (i.e., number of activities) within a 5° × 5° grid during the autumn rainy season between P1 and P2 (P2 minus P1). It also shows the mean position of the WNPSH. The TC track frequency is calculated as the percentage difference, normalized by the total number of the TC genesis over the western North Pacific in P1 and P2, based on the sum of TC track frequency in each grid. The most notable change is a reduction in the TC track frequency by more than 12% (exceed the 90% confidence levels) near the Philippine Sea. The frequency also decreases around Japan on the northward track of TCs from the Philippine Sea. In contrast, the TC track frequency increases over the East China Sea and the Korean Peninsula. Overall, TC tracks shift westward across the western North Pacific. KMA statistics show that the number of TCs making landfall in Korea increases from 2.3 per decade in P1 to 3.2 per decade in P2.

Given the TC movements along the edges of the WNPSH (Choi and Kim, 2019; Ho et al., 2025; Wang and Wang, 2019), the TC track changes from P1 to P2 suggest that the large-scale conditions over the western North Pacific are different between these two periods. The 5870 gpm lines in Fig. 7 indicate that the WNPSH in P2 (solid line) is extended more toward the Asian continent (10°–12° westward) than in P1 (dashed line). While the WNPSH typically retreats toward the central Pacific in September and October, the 5870 gpm lines in P1 and P2 suggest that the retreat of WNPSH in P2 is less pronounced than in P1. The resulting sustained extent of the WNPSH in P2 induces a westward shifts of TC tracks to increase TC influences on Korea in the early autumn period compared to P1.

Factors other than the change in TC tracks—TC intensity, translation speed, and duration—can also contribute to the increased TC-induced rainfall in recent decades. However, there has been no notable change in TC intensities over the past 45 years on the Korean Peninsula (not shown) that can explain the change in the TC-induced rainfall. TC intensities may vary, but it is difficult to directly relate the variations TC intensities to the TC-induced rainfall variations (Feng and Shu, 2018; Ge et al., 2010; Kim et al., 2019; Touma et al., 2019). Similarly, changes in the translation speed and the duration of TCs affecting Korea are not clear (not shown).

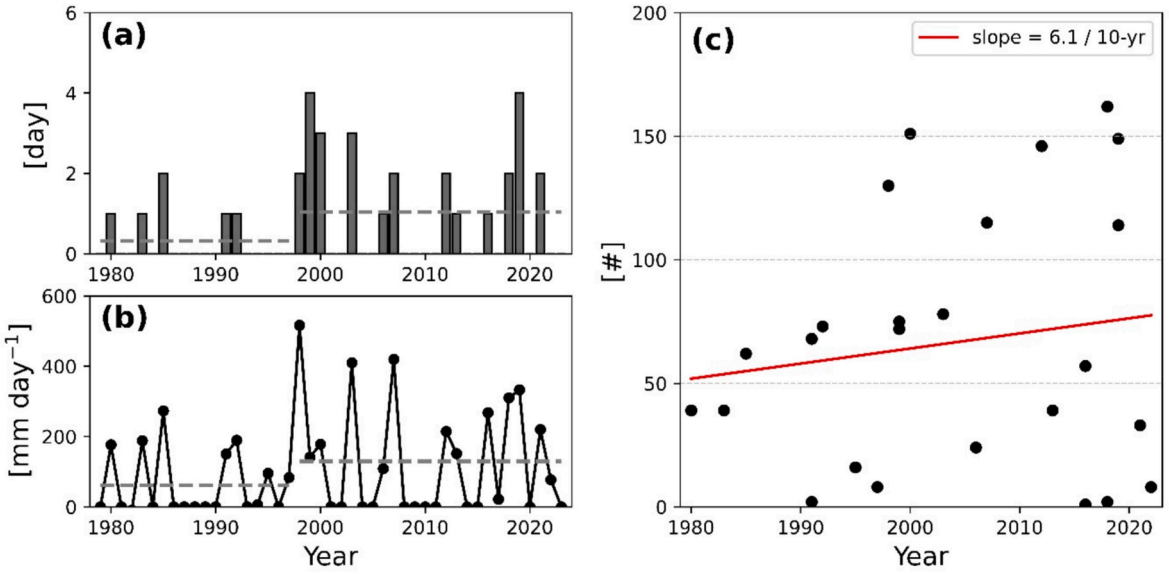


Fig. 6. (a) Number of TC-induced heavy rainfall days ($\geq$ 100 mm day^{-1}), (b) the maximum daily TC-induced rainfall, and (c) the number of TC-affected stations at 61 stations during the autumn rainy season from 1979 to 2023. The dashed horizontal lines in (a) and (b) indicate the mean values for the P1 and P2 periods. The red line in (c) represent the change rate of TC-affected stations. Statistical significance was assessed at the 90% confidence level based on a two-sided Student's *t*-test for the mean differences and the slope of the linear regression. (For interpretation of the references to colour in this figure legend, the reader is referred to the web version of this article.)

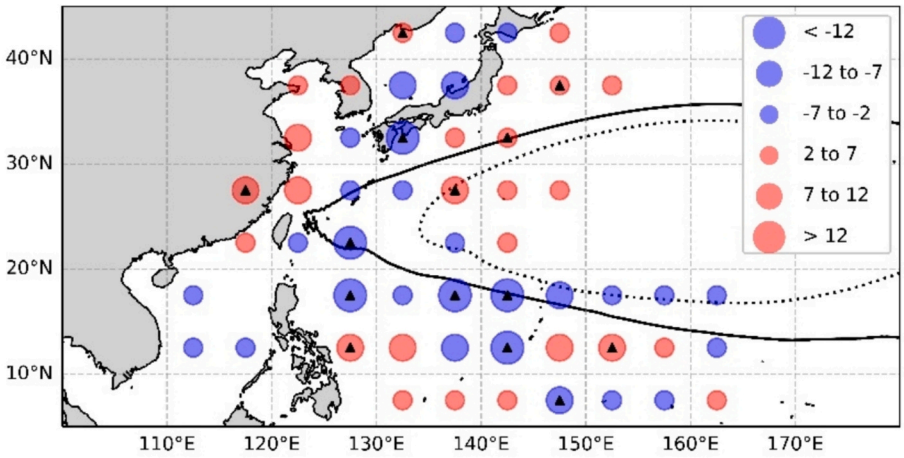


Fig. 7. Differences in TC activity (colour, unit: %) between periods P1 and P2 (P2 minus P1) and the mean position of 5870 gpm contour (dashed for P1, solid for P2) during the autumn rainy season. More (less) TC activity is shown in red (blue). Triangles are enclosed to indicate regions where the changes are statistically significant at the 90% confidence level based on a two-sided Student's *t*-test. In this analysis, each TC is counted only once per 5° × 5° grid, regardless of the duration of its presence or any return passages through the same grid. (For interpretation of the references to colour in this figure legend, the reader is referred to the web version of this article.)

The recent westward movement of TC tracks reasonably explains the increased TC-related rainfall in Korea and the expansion of the TC-affected area during the autumn rainy season. However, frequent occurrence of TC-induced heavy rainfall events cannot be fully explained by the higher frequency of TC approaches alone. Therefore, the climatological changes in the surrounding atmospheric environment that could have affected TC activities are examined. The analysis presented in Fig. 8 focuses on the period from two days before (T_0–2d) to the onset of TC impact in Korea (T_0).

Figs. 8a–c illustrate the differences in SST (shading), 850-hPa moisture flux (vectors), and VIMFD (contours) between P1 and P2 (P2 minus P1), which are critical environmental factors that influence TC-induced rainfall intensity (Chen et al., 2010; Choi et al., 2019; Ge et al., 2010; Kim et al., 2006; Lin et al., 2015; Park et al., 2024). Warmer sea surfaces and a more humid environment in the midlatitudes provide substantial energy for TCs and enable them to maintain their structures over long periods (e.g., Emanuel, 2005; Hill and Lackmann, 2009; Jiang et al., 2008; Powell, 1987; Webster et al., 2005). The figures show general increases in SST in the study area (10°–45°N, 100°–150°E) and lower-level moisture transport from the high SST region toward the TC zone; we identify the TC zone as the area where the moisture flux vectors exhibit distinct cyclonic rotation. In particular, SST increases of over 0.5 °C appear north of 30°N in the western North Pacific, as well as in the East China Sea and the South China Sea. This SST increase is accompanied by enhanced moisture transport from other high-SST regions into TC zones as TCs progress from T_0–2d to T_0.

On the day T_0 − 2d, moisture influx from the South China Sea is especially prominent (Fig. 8a). Weak divergence of vertically integrated moisture flux appears over the South China Sea, accompanied by divergence over Korea. Although it is difficult to directly link SST

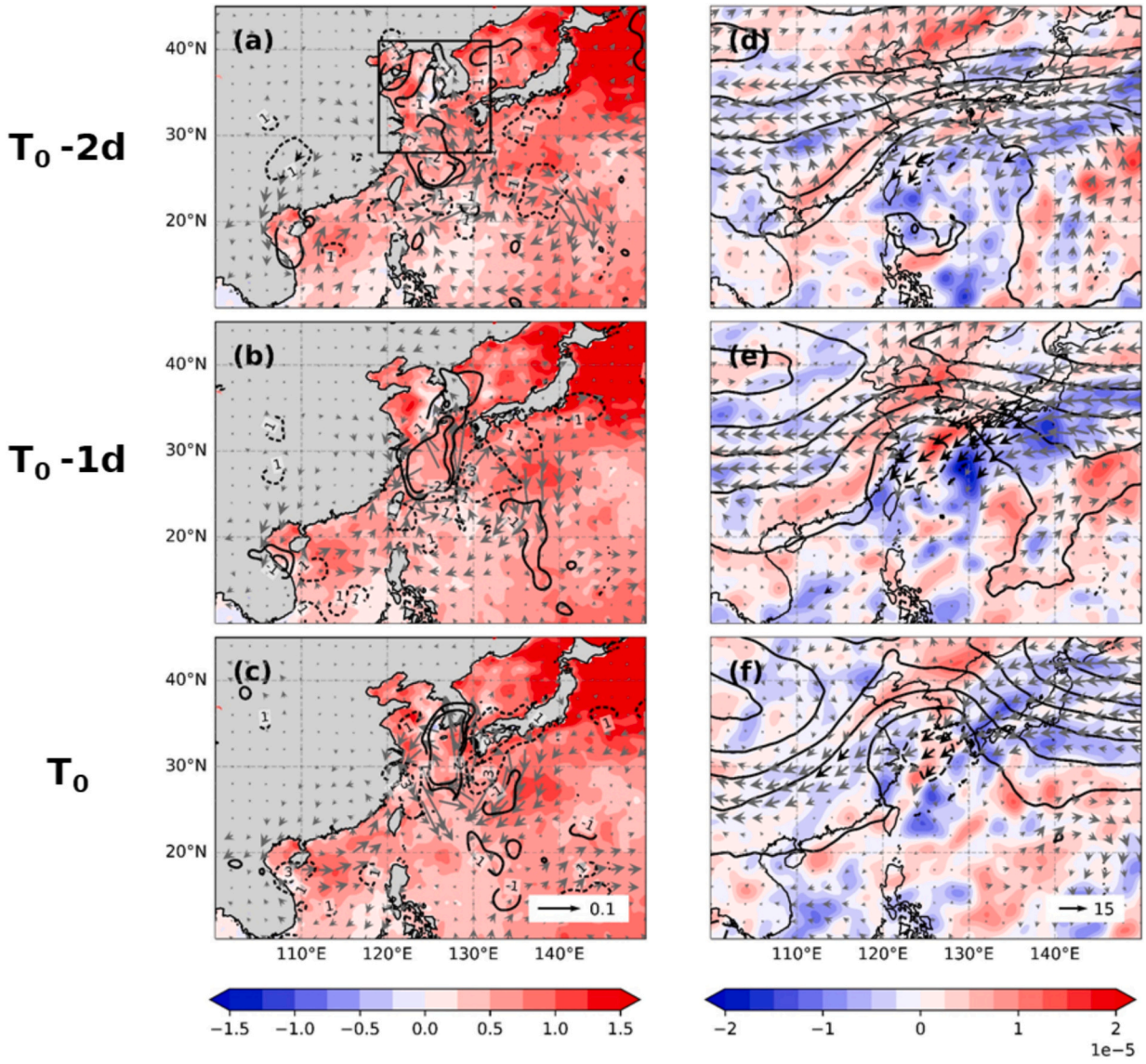


Fig. 8. (a) Differences (P2 minus P1) in (a)–(c) sea surface temperature (shading, unit: K), 850-hPa moisture flux (vectors, unit: m s^{-1}), and vertically integrated moisture flux divergence (contours, unit: 10^{-4} kg m^{-2} s^{-1}), and for (d)–(f) 200-hPa horizontal wind (vectors, unit: m s^{-1}), its divergence (shading, unit: 10^{-5} s^{-1}), and geopotential heights (contour, unit: m). The analysis covers the period two days before (T_0 − 2d), one day before (T_0 − 1d), and the start of TC influence in Korea (T_0). The statistically significant differences, based on a two-sided Student's *t*-test at the 90% confidence level, are highlighted with thick black arrows for moisture flux and horizontal winds. In (a)–(c), solid (dashed) contour lines indicate divergence (convergence) of vertically integrated moisture flux. In (d)–(f), solid (dashed) contour lines represent increase (decrease) in 200-hPa geopotential height. The black rectangular box in (a) marks the TC emergency zone.

increases and moisture transport from the South China Sea to TC-induced rainfall in Korea, several studies suggest potential connections (Byun and Lee, 2012; Park et al., 2011). Park et al. (2011) demonstrated that westerly flows originating in the South China Sea can influence the tracks of recurving TCs heading toward Korea. Similarly, Byun and Lee (2012) showed that moisture from the South China Sea is transported to Korea via a low-level jet, creating favorable conditions for heavy rainfall. They also noted that TCs located near the Taiwan Strait can trigger intense rainfall in Korea. In such cases, elevated SSTs in the South China Sea may provide heat and moisture to TCs passing near Taiwan, potentially helping to maintain their structure during their approach to Korea. While these studies indirectly hint at a connection between the South China Sea and the TCs affecting Korea, further studies are needed to establish this relationship more definitively.

As the TCs move northward closer to Korea in before T_0–1d and T_0 (Fig. 8b and c, respectively), moisture transport from the North Pacific becomes more pronounced and continues as the TCs enter the TC emergency zone. SSTs north of 30°N in the western North Pacific increase by more than 1 °C, which may also contribute to the increase in the intense TC-associated rainfall. The autumn SST increase in the region alters the meridional temperature gradient in the lower troposphere to induce anomalous anticyclonic circulation, resulting in enhanced warm advection into East Asia (Geng et al., 2022). These changes, in conjunction with enhanced low-tropospheric moisture flux and increased SSTs, play a significant role in the intensification of the TC-induced heavy rainfall.

In addition to the heat and moisture supplies in the lower troposphere, upper atmospheric conditions that can promote strong vertical motion within TCs are crucial for intensifying TC-induced rainfall (Kim et al., 2006). The upper-tropospheric divergence, coupled with the low-tropospheric convergence, provides an environment favorable to the sustained development of TCs. To investigate the role of upper tropospheric circulation in the intensification of autumn TCs and associated rainfall, the change in 200-hPa winds and geopotential heights between

P1 and P2 (P2 minus P1) is analyzed (Figs. 8d–f). The most notable change in these figures is the divergence of upper-level horizontal winds over the TC region. In particular, during T_0–1d and T_0, westerly winds within the TC zone weaken significantly ($\geq$ 90% confidence level), and upper-level wind divergence is maintained near the TC center, suggesting a sustained and organized TC structure. Two possible mechanisms may explain this weakening of westerly winds.

First, the weaker westerly winds over the Asian continent and the Korean Peninsula may reflect the weakening of the jet stream. Previous studies documented a long-term weakening trend in the jet stream (Archer and Caldeira, 2008; Kwon et al., 2007; Zhu et al., 2011), which is suggested to influence TC tracks and TC-induced rainfall (Basconcillo and Moon, 2022). According to Basconcillo and Moon (2022), anomalous upper-level easterlies associated with contiguous warm North Pacific SST anomalies contribute to the weakening of the jet streams, which in turn facilitates the northward and westward expansion of the WNPSH. In addition, Park et al. (2011) demonstrated that the weakening of the jet stream over the Asian continent can lead to the formation of a relative jet entrance near the Korean Peninsula, resulting in enhanced upper-tropospheric divergence and lower-tropospheric convergence, both of which promote increased TC-induced rainfall (Kim et al., 2006).

Second, the attenuation of midlatitude westerlies, potentially linked to a weakened jet.

stream within the TC region, can be interpreted as reduction of the vertical wind shear, which facilitates the vertical development of TCs. Decreased vertical wind shear allows TCs to maintain their structure and sustain convection, and delay dissipation. Consequently, TCs approaching Korea may persist longer, increasing the likelihood to bring heavy rainfall in the region. Further supporting this mechanism, Fig. 8e and f show decreases in the 200-hPa geopotential height over the TC area during P2, indicating enhanced vertical developments of TCs.

While it remains difficult to determine whether one of these mechanisms dominates or both act in combination to produce the changes in Figs. 8d–f, the results highlight the crucial role of upper-tropospheric wind divergence in prolonging TC lifespans and enhancing TC-induced heavy rainfall. Specifically, the overlap between upper-tropospheric divergence and lower-tropospheric heat and moisture convergence creates an exceptionally favorable environment for TCs to transport large amount of water vapor and cause heavy rainfall.

5. Conclusion

This study examines recent shift in Korea's rainfall seasonality, marked by the emergence of an autumn rainy season characterized by increased TC-induced rainfall. A comparison between the P1 and P2 periods reveals that since 1997/1998, the average daily rainfall from September 10 to October 10 increased by 1.8 mm day^{-1}, accompanied by larger frequency of heavy rainfall days. Among various contributing factors, TC-induced rainfall plays the most substantial role, accounting for approximately 72% of the total increase in rainfall during this period. The strong contribution is further supported by a strong interannual correlation (R) of 0.78 between total rainfall and TC-induced rainfall during the autumn rainy season. The non-TC rainfall remains nearly unchanged from P1 to P2 (not shown) and thus are not related to the autumn rainy period.

A key driver of this phenomenon is the westward shift of the TC tracks to result in more frequent and prolonged TC influences over Korea in early autumn. This shift is closely related to the delayed retreat of the WNPSH, which extends further west in P2 than in P1. The WNPSH typically guides TCs along its southwestern periphery via steering flows. When its retreat in autumn is delayed, TCs are more likely to recurve toward the East China Sea and Korea, instead of veering northeastward away from the region. As a result, the area affected by TCs over Korea expands, and the amount of TC-induced rainfall increases. In addition, warmer SSTs in the surrounding seas, including the western North Pacific and South China Sea, in conjunction with enhanced low-level moisture transport from high-SST regions, provide large amount of energy to enhance the TC-induced rainfall. Furthermore, weakening of the westerly winds over the TC region associated with jet stream weakening or reduced vertical wind shear in the TC environment, also works to increase upper-tropospheric divergence. These changes provide a favorable condition for enhancing the interaction between the upper-tropospheric divergence and lower-tropospheric convergence, to further intensify the TC-induced rainfall in Korea.

When discussing the impact of increased autumn rainfall due to TC activities, it is important to consider not only the meteorological phenomenon itself but also its societal and economic consequences. The more frequent occurrence of heavy rainfall events and the expansion of the area affected by TC-induced rainfall are directly related to increased damages in various sectors, particularly in agriculture and crop production. (MOIS, 2024). Although agriculture accounts for a smaller share of the Korean economy than other sectors, its societal and economic impacts remain significant in Korea. To mitigate these risks and reduce potential losses, it is essential to raise public awareness and implement effective government policy measures. The development of detailed adaptation strategies would also benefit from expert input by scientists in relevant fields.

Given the societal and economic importance of the autumn rainy season, a careful and quantitative approach to its management is required. To enable effective policy responses, it is essential to define the season in a scientifically clear manner, which involves detailed analyses of both TC- and non-TC-induced rainfall. Diagnostic experiments are also necessary to quantitatively assess the roles of environmental factors such as SST and moisture flux associated with changes in TC activity.

Building on these efforts, future research should aim to project the changes in autumn rainfall under future climate. Assessments based on the Coupled Model Intercomparison Project Phase 6 (CMIP6) using various Shared Socioeconomic Pathways (SSPs) would provide a more detailed evaluation of autumn rainfall variability driven by climate change. Such efforts will contribute to deeper understanding of future climatic risks and support the development of strategies to mitigate their adverse societal and environmental impacts.

CRediT authorship contribution statement

Hee-Ae Kim: Writing – review & editing, Writing – original draft, Visualization, Investigation, Formal analysis, Conceptualization. **Chang-Hoi Ho:** Writing – review & editing, Supervision, Funding acquisition, Conceptualization. **Minhee Chang:** Writing – review & editing, Formal analysis. **Jinwon Kim:** Writing – review & editing, Formal analysis.

Declaration of competing interest

The authors declare that they have no known competing financial interests or personal relationships that could have appeared to influence the work reported in this paper.

Acknowledgements

We would like to thank three anonymous reviewers for their helpful comments. This study was funded by the Korea Meteorological Administration Research and Development Program under Grant RS-2023-00236880 and was also supported by the Specialized University Program of the Korea Meteorological Institute (KMI). The funders played no role in study design, data collection, analysis and interpretation of data, or the writing of this manuscript.

Data availability

The authors do not have permission to share data.

References

Archer, C.L., Caldeira, K., 2008. Historical trends in the jet streams. Geophys. Res. Lett. 35, L08803. https://doi.org/10.1029/2008GL033614.

Basconcillo, J., Moon, I.-J., 2022. Increasing activity of tropical cyclones in East Asia during the mature boreal autumn linked to long-term climate variability. npj Clim. Atmos. Sci. 5, 4. https://doi.org/10.1038/s41612-021-00222-6.

Byun, K.-Y., Lee, T.-Y., 2012. Remote effects of tropical cyclones on heavy rainfall over the Korean peninsula–statistical and composite analysis. Tellus A: Dyn. Meteorol. Oceanogr. 64, 14983. https://doi.org/10.3402/tellusa.v64i0.14983.

Chan, J.C., 2000. Tropical cyclone activity over the western North Pacific associated with El Niño and La Niña events. J. Clim. 13, 2960–2972. https://doi.org/10.1175/1520-0442(2000)013<2960:TCAOTW>2.0.CO;2.

Chand, S.S., Walsh, K.J.E., Camargo, S.J., Kossin, J.P., Tory, K.J., Wehner, M.F., Chan, J. C.L., Klotzbach, P.J., Dowdy, A.J., Bell, S.S., Ramsay, H.A., Murakami, H., 2022. Declining tropical cyclone frequency under global warming. Nat. Clim. Chang. 12, 655–661. https://doi.org/10.1038/s41558-022-01388-4.

Chang, M., Ho, C.-H., Ho, J., Cha, E.-J., 2023. Centennial analysis in tropical cyclone-induced precipitation in Korea. Weather Clim. Extrem. 39, 100549. https://doi.org/10.1016/j.wace.2023.100549.

Chen, L., Li, Y., Cheng, Z., 2010. An overview of research and forecasting on rainfall associated with landfalling tropical cyclones. Adv. Atmos. Sci. 27, 967–976. https://doi.org/10.1007/s00376-010-8171-y.

Choi, W., Kim, K.-Y., 2019. Summertime variability of the western North Pacific subtropical high and its synoptic influences on the East Asian weather. Sci. Rep. 9, 7865. https://doi.org/10.1038/s41598-019-44414-w.

Choi, K.-S., Moon, J.-Y., Kim, D.-W., Byun, H.-R., Kripalani, R.H., 2010. The significant increase of summer rainfall occurring in Korea from 1998. Theor. Appl. Climatol. 102, 275–286. https://doi.org/10.1007/s00704-010-0256-0.

Choi, W., Ho, C.-H., Kim, M.-K., Kim, J., Yoo, H.-D., Jhun, J.-G., Jeong, J.-H., 2018. Season-dependent warming characteristics observed at 12 stations in South Korea over the recent 100 years. Int. J. Climatol. 38, 4092–4101. https://doi.org/10.1002/joc.5554.

Choi, J., Lee, J., Kim, S., 2019. Impact of sea surface temperature and surface air temperature on maximizing typhoon rainfall: focusing on typhoon Maemi in Korea. Adv. Meteorol. 2019, 1930453. https://doi.org/10.1155/2019/1930453.

Do, H.-S., Kim, J., Cha, E.-J., Chang, E.-C., Son, S.-W.L., Lee, G., 2023. Long-term change of summer mean and extreme precipitations in Korea and East Asia. Int. J. Climatol. 43, 3476–3492. https://doi.org/10.1002/joc.8039.

Donat, M.G., Pardowitz, T., Leckebusch, G.C., Ulbrich, U., Burghoff, O., 2011. High-resolution refinement of a storm loss model and estimation of return periods of loss-intensive storms over Germany. Nat. Hazards Earth Syst. Sci. 11, 2821–2833. https://doi.org/10.5194/nhess-11-2821-201.

Emanuel, K., 2005. Increasing destructiveness of tropical cyclones over the past 30 years. Nature 436, 686–688. https://doi.org/10.1038/nature03906.

Feng, X., Shu, S., 2018. How do weak tropical cyclones produce heavy rainfall when making landfall over China. J. Geophys. Res. Atmos. 123, 11830–11848. https://doi.org/10.1029/2018JD029228.

Ge, X., Li, T., Zhang, S., Peng, M., 2010. What causes the extremely heavy rainfall in Taiwan during Typhoon Morakot (2009)? Atmos. Sci. Lett. 11, 46–50. https://doi.org/10.1002/asl.255.

Geng, Y., Ren, H.L., Ma, X., Zhao, S., Nie, Y., 2022. Responses of East Asian climate to SST anomalies in the Kuroshio Extension region during boreal autumn. J. Clim. 35, 7007–7023. https://doi.org/10.1175/JCLI-D-21-0711.1.

Hill, K.A., Lackmann, G.M., 2009. Influence of environmental humidity on tropical cyclone size. Mon. Weather Rev. 137, 3294–3315. https://doi.org/10.1175/2009MWR2679.1.

Ho, C.-H., Kang, I.-S., 1988. The variability of precipitation in Korea. Asia-Pac. J. Atmos. Sci. 24, 38–48 (in Korean).

Ho, C.-H., Baik, J.-J., Kim, J.-H., Gong, D.-Y., Sui, C.-H., 2004. Interdecadal changes in summertime typhoon tracks. J. Clim. 17, 1767–1776. https://doi.org/10.1175/1520-0442(2004)017<1767:ICISTT>2.0.CO;2.

Ho, C.-H., Kim, H.-A., Cha, Y., Do, H.-S., Kim, J., Kim, J., Kim, J., Park, S.K., Yoo, H.-D., 2025. Recent changes in summer rainfall characteristics in Korea. J. Eur. Meteorol. Soc. 2, 100009. https://doi.org/10.1016/j.jemets.2025.100009.

Jiang, H., Halverson, J.B., Zipser, E.J., 2008. Influence of environmental moisture on TRMM-derived tropical cyclone precipitation over land and ocean. Geophys. Res. Lett. 35, L17806. https://doi.org/10.1029/2008GL034658.

Kim, J.-H., Ho, C.-H., Sui, C.-H., 2005. Circulation features associated with the record-breaking typhoon landfall on Japan in 2004. Geophys. Res. Lett. 32, L14713. https://doi.org/10.1029/2005GL022494.

Kim, J.-H., Ho, C.-H., Lee, M.-H., Jeong, J.-H., Chen, D., 2006. Large increase in heavy rainfall associated with tropical cyclone landfalls in Korea after the late 1970s. Geophys. Res. Lett. 33, L18706. https://doi.org/10.1029/2006GL027430.

Kim, T., Shin, J.-Y., Kim, S., Heo, J.-H., 2018. Identification of relationships between climate indices and long-term precipitation in South Korea using ensemble empirical mode decomposition. J. Hydrol. 557, 726–739. https://doi.org/10.1016/j.jhydrol.2017.12.069.

Kim, D., Ho, C.-H., Park, D.-S.R., Kim, J., 2019. Influence of vertical wind shear on wind- and rainfall areas of tropical cyclones making landfall over South Korea. PLoS One 14, e0209885. https://doi.org/10.1371/journal.pone.0209885.

Knutson, T., Camargo, S.J., Chan, J.C.L., Emanuel, K., Ho, C.-H., Kossin, J., Mohapatra, M., Satoh, M., Sugi, M., Walsh, K., Wu, L., 2020. Tropical cyclones and climate change assessment: Part II: projected response to anthropogenic warming. Bull. Am. Meterol. Soc. 101, E303–E322. https://doi.org/10.1175/BAMS-D-18-0194.1.

Kwon, M., Jhun, J.-G., Ha, K.-J., 2007. Decadal change in east Asian summer monsoon circulation in the mid-1990s. Geophys. Res. Lett. 34, L21706. https://doi.org/10.1029/2007GL031977.

Lin, Y., Zhao, M., Zhang, M., 2015. Tropical cyclone rainfall area controlled by relative sea surface temperature. Nat. Commun. 6, 6591. https://doi.org/10.1038/ncomms7591.

Ministry of the Interior and Safety (MOIS), 2024. Natural Disaster Yearbook 2023. https://www.mois.go.kr/frt/bbs/type001/commonSelectBoardArticle.do;jsessionid=ECqStMLfatIIZCE7Z+pMHEMX.node10?bbsId=BBSMSTR_000000000014&nttId=114838 (in Korean).

Moon, J.-Y., Park, C.-Y., Choi, Y.-E., 2011. Changes in the characteristics of summer rainfall caused by the regime shift in the Republic of Korea. J. Kor. Geogr. Soc. 46, 277–290 (in Korean).

Na, H., Jung, W.-S., 2020. Autumn typhoon affecting the Korean Peninsula–past and present characteristics. J. Korean Soc. Atmos. Environ. 36, 482–491 (in Korean).

Nakamura, J., Camargo, S.J., Sobel, A.H., Henderson, N., Emanuel, K.A., Kumar, A., LaRow, T.E., Murakami, H., Roberts, M.J., Scoccimarro, E., Vidale, P.L., Wang, H., Wehner, M.F., Zhao, M., 2017. Western North Pacific tropical cyclone model tracks in present and future climates. J. Geophys. Res. Atmos. 122, 9721–9744. https://doi.org/10.1002/2017JD027007.

Park, D.-S.R., Ho, C.-H., Kim, J.-H., 2014. Growing threat of intense tropical cyclones to East Asia over the period 1977–2010. Environ. Res. Lett. 9, 014008. https://doi.org/10.1088/1748-9326/9/1/014008.

Park, D.-S.R., Ho, C.-H., Kim, J.-H., Kim, H.-S., 2011. Strong landfall typhoons in Korea and Japan in a recent decade. J. Geophys. Res. Atmos. 116, D07105. https://doi.org/10.1029/2010JD014801.

Park, D.-S.R., Ho, C.-H., Nam, C.C., Kim, H.-S., 2015. Evidence of reduced vulnerability to tropical cyclones in the Republic of Korea. Environ. Res. Lett. 10, 054003. https://doi.org/10.1088/1748-9326/10/5/054003.

Park, D.-S.R., Seo, E., Lee, M., Cha, D.-H., Kim, D., Ho, C.-H., Lee, M.-I., Kim, H.-S., Min, S.-K., 2024. Sea surface temperature warming to inhibit mitigation of tropical cyclone destructiveness over East Asia in El Niño. npj Clim. Atmos. Sci. 7, 24.

Powell, M.D., 1987. Changes in the low-level kinematic and thermodynamic structure of Hurricane Alicia (1983) at landfall. Mon. Weather Rev. 115, 75–99. https://doi.org/10.1175/1520-0493(1987)115<0075:CITLLK>2.0.CO;2.

Qian, W., Kang, H.-S., Lee, D.-K., 2002. Distribution of seasonal rainfall in the East Asian monsoon region. Theor. Appl. Climatol. 73, 151–168. https://doi.org/10.1007/s00704-002-0679-3.

Rha, D.-K., Kwak, C.-H., Suh, M.-S., Hong, Y., 2005. Analysis of the Characteristics of precipitation over South Korea in terms of the associated synoptic patterns: a 30 years climatology (1973~2002). J. Kor. Earth Sci. Soc. 26, 732–743 (in Korean).

Shan, K., Lin, Y., Chu, P.S., Yu, X., Song, F., 2023. Seasonal advance of intense tropical cyclones in a warming climate. Nature 623, 83–89. https://doi.org/10.1038/s41586-023-06544-0.

Sobel, A.H., Camargo, S.J., Hall, T.M., Lee, C.-Y., Tippett, M.K., Wing, A.A., 2016. Human influence on tropical cyclone intensity. Science 353, 242–246. https://doi.org/10.1126/science.aaf6574.

Son, H.-Y., Park, J.-Y., Kug, J.-S., 2016. Precipitation variability in September over the Korean Peninsula during ENSO developing phase. Clim. Dyn. 46, 3419–3430. https://doi.org/10.1007/s00382-015-2776-x.

Touma, D., Stevenson, S., Camargo, S.J., Horton, D.E., Diffenbaugh, N.S., 2019. Variations in the intensity and spatial extent of tropical cyclone precipitation. Geophys. Res. Lett. 46, 13992–14002. https://doi.org/10.1029/2019GL083452.

Wang, C., Wang, B., 2019. Tropical cyclone predictability shaped by western Pacific subtropical high: integration of trans-basin sea surface temperature effects. Clim. Dyn. 53, 2697–2714. https://doi.org/10.1007/s00382-019-04651-1.

Webster, P.J., Holland, G.J., Curry, J.A., Chang, H.-R., 2005. Changes in tropical cyclone number, duration, and intensity in a warming environment. Science 309, 1844–1846. https://doi.org/10.1126/science.1116448.

Wu, L., Wang, B., 2004. Assessing impacts of global warming on tropical cyclone tracks. J. Clim. 17, 1686–1698. https://doi.org/10.1175/1520-0442(2004)017<1686:AIOGWO>2.0.CO;2.

Wu, L., Wang, B., Geng, S., 2005. Growing typhoon influence on East Asia. Geophys. Res. Lett. 32, L18703. https://doi.org/10.1029/2005GL022937.

Wu, Q., Wang, X., Tao, L., 2020. Interannual and interdecadal impact of Western North Pacific Subtropical High on tropical cyclone activity. Clim. Dyn. 54, 2237–2248. https://doi.org/10.1007/s00382-019-05110-7.

Yang, J.-S., 1999. Synoptic climatological characteristics of distribution of precipitation in Korea in early autumn. J. Kor. Assoc. Reg. Geogr. 5, 151–162 (in Korean).

Yao, X., Zhao, D., Li, Y., 2020. Autumn tropical cyclones over the Western North Pacific during 1949-2016: A statistical study. J. Meteorol. Res. 34, 150–162. https://doi.org/10.1007/s13351-020-9019-8.

Zhang, W., Graf, H.F., Leung, Y., Herzog, M., 2012. Different El Niño types and tropical cyclone landfall in East Asia. J. Clim. 25, 6510–6523. https://doi.org/10.1175/JCLI-D-11-00488.1.

Zhao, J., Zhan, R., Wang, Y., 2018. Global warming hiatus contributed to the increased occurrence of intense tropical cyclones in the coastal regions along East Asia. Sci. Rep. 8, 6023. https://doi.org/10.1038/s41598-018-24402-2.

Zhu, Y., Wang, H., Zhou, W., Ma, J., 2011. Recent changes in the summer precipitation pattern in East China and the background circulation. Clim. Dyn. 36, 1463–1473. https://doi.org/10.1007/s00382-010-0852-9.